

Tuning of conversion and optical emission by electron temperature in an inductively-coupled CO₂ plasma

*Diyu Zhang^a, Qiang Huang ^{*a}, Edwin J. Devid^a, Eric Schuler^b, N. Raveendran Shiju^b, Gadi
Rothenberg^b, Gerard van Rooij^c, Ruilong Yang^d, Kezhao Liu^d, and Aart W. Kleyn ^{*a}*

^a Center of Interface Dynamics for Sustainability, Institute of Materials, China Academy of
Engineering Physics, Chengdu, Sichuan 610200, People's Republic of China

^b Van 't Hoff Institute for Molecular Sciences, University of Amsterdam, P.O. Box 94157,
1090 GD Amsterdam, The Netherlands

^c Dutch Institute for Fundamental Energy Research, P.O. Box 6336, 5600 HH Eindhoven, The
Netherlands

^d Science and Technology on Surface Physics and Chemistry Laboratory, P.O. Box 718-35,
Mianyang 621907, People's Republic of China

* Corresponding authors. Email: qhuang1986@163.com. Email: a.w.kleijn@contact.uva.nl

ABSTRACT

This paper focuses on how the electron temperature and other plasma properties affect optical emission and CO₂ conversion in a CO₂ plasma. Such plasma-mediated reactions can enable efficient CO₂ reuse. We study CO₂ and CO plasmas generated by inductively-coupled radiofrequency power (30–300 W) at low pressures (6–400 Pa). By varying the argon admixture, we can study the effect of the electron temperature, T_e , on the conversion and emission properties using optical emission spectroscopy, mass spectrometry and electrical probe measurements. Importantly, we can observe several parameters simultaneously: T_e , CO₂ conversion, chemiluminescence from CO₂ and dissociation products and optical emission from several atomic and CO transitions and from the C₂ Swan system. Based on these results, we establish a correlation between T_e , the CO₂ conversion and the optical emission spectra. A low T_e enhances CO₂ conversion and Swan band emission. In contrast with published studies, our results show that the CO₂ and C₂ vibrations are not in local equilibrium. This means that the vibrational temperatures of CO₂ and C₂ should differ.

KEYWORDS: carbon dioxide, inductively-coupled plasma, optical emission spectroscopy, electron temperature

1. INTRODUCTION

CO₂ capture, storage and utilization are key actions for mitigating climate change. Converting CO₂ into useful products can be done in different ways, including electrocatalysis, thermolysis and plasma reactions¹⁻⁶. But via any thermal route, CO₂ dissociation incurs a hefty thermodynamic penalty. Therefore, non-thermal processes, where energy is transferred to relevant degrees of freedom, such as vibrational excitation, are preferable^{5,7}. Of these, plasma conversion is becoming more and more attractive as the cost of renewable electricity decreases.

There are many ways for generating CO₂ plasma. Here we focus on radiofrequency inductively coupled plasma (RF-ICP). This setup is relatively simple and scalable to high power. It also allows easy access to diagnostics and coupling with catalysts. There are few published examples using RF plasma for CO₂ conversion⁸⁻¹¹. Spencer and Gallimore studied CO₂ conversion in atmospheric RF Ar/CO₂ plasma. They found very high conversion of CO₂, but low energy efficiencies⁹. This low efficiency is not intrinsic to RF plasma. The conversion of electrical power to plasma heating can be as high as 0.95¹². This suggests that there is room for improvement of the energy efficiency, and that RF plasma can become a viable way to convert CO₂.

The direct thermal dissociation of CO₂ requires temperatures above 2400 K, and typically yields a maximum energy efficiency of ca. 50%. Studies on plasma-mediated conversion showed higher energy efficiencies for CO₂ dissociation already in the 1970s⁷. It is a promising route to CO₂ dissociation at low gas temperatures^{5, 13-17}. This is because in a non-thermal plasma the temperatures of various degrees of freedom may differ. These include the neutral gas temperature, the electron temperature (T_e), ion temperature, and temperatures corresponding to the rotational and vibrational degrees of freedom. This allows specific heating of the degrees of freedom that are relevant for CO₂ dissociation. An appropriately chosen

plasma can excite relevant molecular vibrations (such as bending) more than translation and rotation.

There are two ways in which plasma can excite the molecular vibration of CO₂: (1) one step electronic excitation leading to electronically excited states, that subsequently decay. (2) step-wise excitation through low energy electrons exciting CO₂ molecules vibrationally, but in the electronic ground state. The latter process is called ‘ladder climbing’. When two excited molecules collide, the more energetic one gets even more excited while the other falls back to its ground state ^{5, 17-18}. Direct spectroscopic evidence for CO₂ ladder climbing is not available (it was observed for CO and N₂ ¹⁹), but simulations suggest its importance ²⁰. Recently, vibrationally excited CO₂ was observed in a plasma ²¹, but its role in ladder climbing is still a moot point.

The excitation of specific vibrational modes can enhance the dissociation probability of a molecule on a (catalyst) surface. This was proven through laser heating of specific vibrational modes of CH₄ ²². Recently, this work was extended to CO₂ conversion at Ni(100) surfaces ²³. While using lasers for large-scale conversion processes is impossible, plasma excitation with a high electrical efficiency could be a viable option. Indeed, it was suggested recently that non-thermal plasma conversion can form the basis of a CO₂ conversion plant ²⁴.

To gain more insight into the mechanism of CO₂ conversion in non-thermal plasma, we study here how changing plasma conditions affects the CO yield. We do this by changing the electron temperature of the discharge in the presence of Ar. This was demonstrated earlier in the case of an RF N₂ plasma with the addition of He or Ar ²⁵. Besides the CO yield we also study how the change in electron temperature affects the plasma’s optical emission. We find that the emission of C₂ via the Swan bands is strongly correlated with T_e. Interestingly, the suggestion that the CO₂ vibrational temperature can be derived from measurements of Swan band emission ^{9, 26-27} does not hold in our case.

2.1 Experimental set-up

All experiments were carried out by our RF-ICP reactor, as shown in Figure 1. The plasma reactor chamber is made from a quartz glass tube, with diameter of 80 mm and length of 400 mm. It is kept in place by two stainless steel flanges and sealed by O-rings. The reaction chamber is surrounded by a 6-turn copper coil, cooled by flowing water through the copper tube. To establish an efficient coupling of RF energy into the plasma, a matching box is connected to the RF power supply (27.12 MHz, 2 kW) and the coil. The maximum power used was 300 W and the reflected power was kept less than 1 W by the matching box (an unknown amount of power dissipates in the coil). The radiofrequency electromagnetic field was shielded by an aluminum RF Faraday shield. Gases used in the reaction were directly obtained from the connected gas cylinders and mixed before going into the reaction chamber. Each gas cylinder was equipped with a calibrated mass flow controller (MFC, Sevenstar D07-19B). The plasma ignites inside the tube after supplying RF power. The reaction chamber was evacuated by a vacuum pump system with two stage pumping (Roots pump and rotary pump) with the nominal pumping speed around $350 \text{ m}^3\text{h}^{-1}$. The pumping speed can be reduced by a throttle valve.

Prior to feeding the reaction gases, the reactor chamber was evacuated to 10^{-1} Pa. The CO_2 (99.999%) dissociation experiments were carried out at different specific supplied power (from 30 W to 300 W) and flow rates (10, to 100 Standard Cubic Centimeter per Minute, hereafter denoted as sccm). When CO_2 was mixed with Ar, the Ar (99.999%) flow rate was fixed at 100 or 1000 sccm. Undiluted CO_2 or CO (99.9%) plasma was respectively generated at a gas flow of 100 to 200 sccm. The operation pressure could be varied by the throttle valve. Pressures ranged from 10 to 200 Pa and are listed for all data presented. The parameter space of the experiments is large; therefore, we have to compare experiments done under slightly different conditions of flow, pressure, and power.

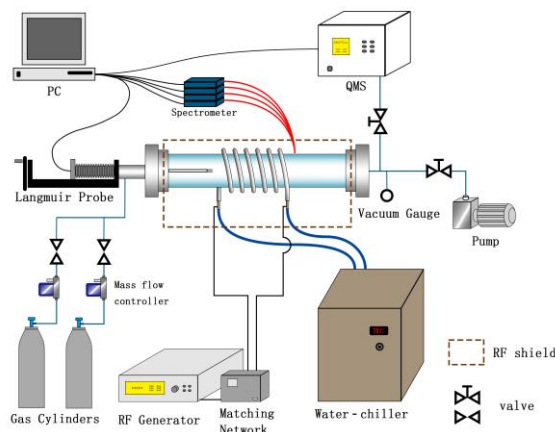


Figure 1. Schematic diagram of experimental setup. See text for details.

The optical emission of plasma was monitored using an optical fiber cable placed at downstream location 1.5cm from the coil (Figure 1) and viewing the center of the plasma. The data was transmitted to our UV-VIS-NIR spectrometers (spectrometer, StellarNet LSR-NIR3b, LSR-UV2, LSR-VIS4b and LSR-VIS4). For comparing the OES from different channels, the intensity of spectra has been presented in a normalized unit, counts per second, which is the same for all spectra. The wavelength observed in our experiment is at most 0.5 nm off the literature values. We attribute this to the limited accuracy in the wave length scale of the spectrometers.

A differentially pumped quadrupole mass spectrometer (QMS, Hiden HPR20) was connected to the reactor for carbon dioxide conversion measurements. It was equipped with a variable leak valve to let the gasses into the QMS. To evaluate the amount of different gases in the ICP reactor quantitatively, the data obtained from the QMS were carefully corrected following the calibration method given in references ^{26, 28}.

A double pin Langmuir probe (Double probe, Impedans Inc.) was used to measure the electron temperature (T_e) and the ion density (n_i) in the plasma. The distance between the Langmuir probe pins and the coil was 5 cm. The probe could not be moved during experiments.

However, by visual inspection we verified that the probe was in the center of the plasma on the upstream side. This probe is sensitive to the RF field in the plasma. Therefore, we ran measurements with the Langmuir double probe. These measurements do not give the whole electron energy distribution function (EEDF), but only T_e and n_i . Analysis was done using the expressions of Rousseau et al., which is very similar to those of the earlier work by Chang and Laframboise²⁹⁻³⁰. The maximum pressure for which the analysis is claimed to be correct is more than 10 Torr, 1330 Pa. A Maxwellian electron energy distribution function is assumed, which is found reasonable by Singh and Graves³¹. We note that the ion density measurement corresponds to some average density of the ions involved, CO_2^+ and Ar^+ or N_2^+ and Ar^+ . Thus, we cannot draw any firm conclusions from n_i and do not show any measurements.

2.2 Spectroscopy

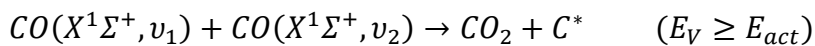
Optical emission spectroscopy (OES) is a non-invasive measurement method and widely used on real-time monitoring of the plasma to identify the chemical components and various parameters (e.g. electron temperature, electron density, gas pressure), see for recent entries into the literature^{27, 32-34}. Although the concentration of radiating molecules in the plasma is very low (4-6 orders lower than neutral gas density) several bands and lines have been identified in the visible spectral region from 450 – 855 nm. A CO or CO_2 plasma shows a strong continuous spectral background, due to the chemiluminescence from the recombination of CO and O³⁵⁻³⁶. In the process CO_2 $^3\text{B}_2$, $^1\text{B}_2$, and $^1\Sigma\text{g}^+$ are formed. This broad frequency spectrum is hard to analyze. Rond et al. made a crude estimate of the absolute intensities which discards the spectroscopic fine structure. Such and more detailed analysis are not required for the present work³⁷. The chemiluminescence spectrum is usually subtracted from the superimposed sharper spectral features³⁷.

Table 1. CO and C₂ transitions observed in this study.

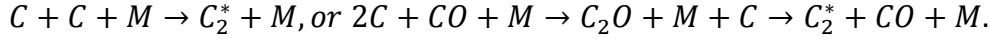
Molecular	Transitions	Upper state (eV)	lower state (eV)	ΔE (eV)
CO	Ångstrom	10.78	8.07	2.71
	(B ¹ Σ ⁺ → A ¹ Π)			
	3 rd positive system	10.39	6.04	4.35
	(b ³ Σ ⁺ → a ³ Π _r)			
CO	Asundi	6.92	6.04	0.88
	(a' ³ Σ ⁺ → a ³ Π _r)			
CO	Triplet	7.58	6.04	1.54
	(d ³ Δ → a ³ Π _r)			
C ₂	Swan band	2.48	0.09	2.39
	(d ³ Π _g → a ³ Π _u)			

CO emits in the range of 450 – 855 nm through 3 bands: Ångstrom, Asundi and Triplet. In addition, we used lines of the CO 3rd positive system at 283 nm. The characteristics of the bands used are listed in Table 1. It is important to note that the excitation energy of the upper states of these transitions requires 6 – 11 eV of energy, involving fairly hot electrons for excitation ³⁸.

The C₂ Swan band requires a much lower excitation energy, around 2 eV and its emission can be expected in plasma with lower T_e. However, the C₂ molecule should be produced first before it can be electronically excited and radiate. The formation process in CO gas has been studied by Wallaart et al. ³⁹. At first C* atoms are generated in vibration-enhanced CO collisions:



Here the vibrational energy in the molecules E_v should exceed the activation energy for reaction E_{act} . Subsequently, molecular C_2 can be produced in two ways: direct recombination of carbon atoms with help of a third body (M) or in reactions involving C_2O , such as:



The C_2 formation probability will be proportional to the CO concentration as the power 2 or more. Detailed modelling of the C_2 emission spectrum is beyond the scope of the present paper. In fact, any complete modelling of C_2 formation in a reactive plasma is not available to the knowledge of the authors.

Many groups studied carbon dioxide dissociation by OES^{26-27, 33, 37}. Strong optical emission of CO and C_2 Swan band emission has been observed in CO_2 plasma^{26-27, 37, 40}. The optical emission of the C_2 Swan band was mainly generated by microwave plasma at near atmospheric pressure²⁶⁻²⁷.

Besides molecular emission, a number of atomic lines of O, C and additional atomic gasses in the plasma such as Ar, can be expected. This emission was observed in many studies, and we will discuss it only briefly here.

3. RESULTS

3.1 Electron temperature

Figure 2a shows the dependence on power of T_e for pure Ar or CO_2 plasma. We notice that T_e of CO_2 plasma slightly decreases with increasing power. These trends agree with the results of Younus et al., Hopwood et al. and Godyak et al. for an ICP⁴¹⁻⁴³, as well as those of Nisha et al. and Vargheese et al.⁴⁴⁻⁴⁵ for different plasmas. As the geometries and conditions of these experiments vary, we can only compare trends.

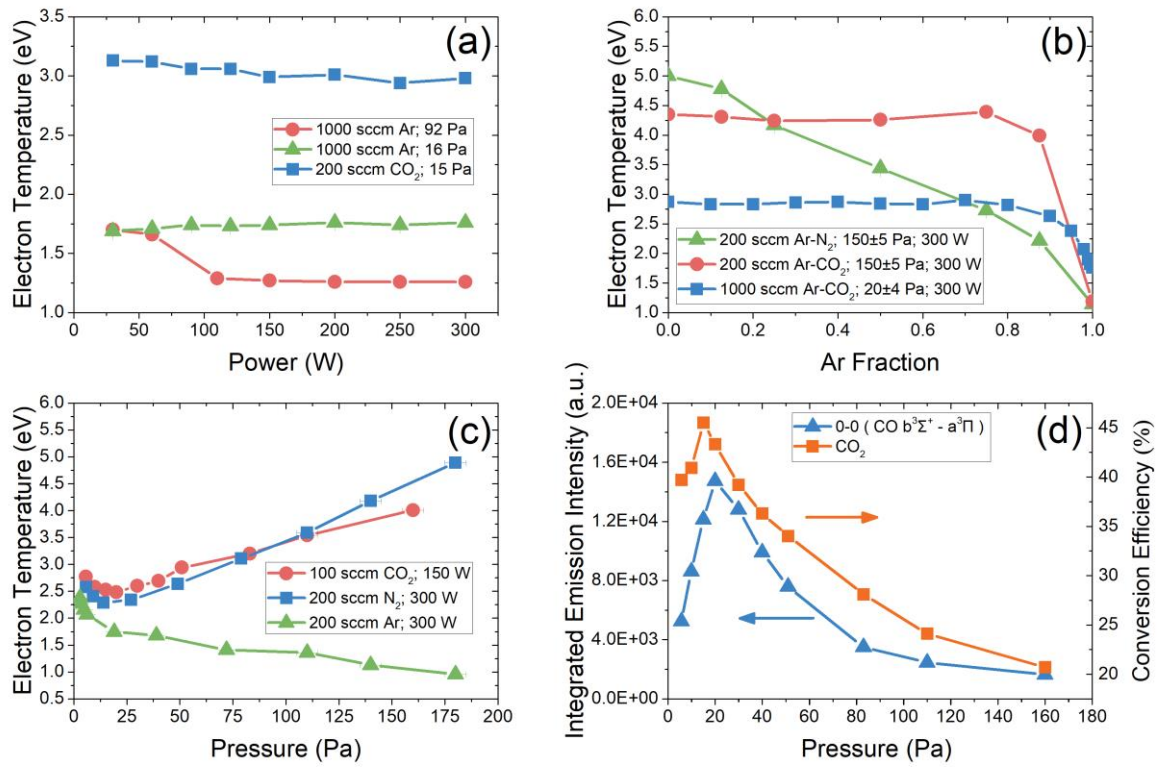


Figure 2. (a) Measurements of the electron temperature (T_e) in pure Ar or CO₂ plasma as a function of the power, for various pressures and gas flows indicated in the figure.

(b) T_e dependence on Ar/(Ar+X) flow ratio, where X= N₂ or CO₂. The pressures and flow rates are indicated in the figure. Power was fixed at 300 W. The X flow rate was adjusted to obtain the ratio required.

(c) Dependence of T_e on reactor pressure for pure plasma of Ar, CO₂ and N₂. Conditions are indicated in the figure.

(d) Dependences of conversion efficiency and emission intensity of the CO ($b^3\Sigma^+ - a^3\Pi$) 0-0 on reactor pressure. The CO₂ flow was fixed at 100 sccm. Power was fixed at 150 W.

Figure 2b shows the dependence of T_e on the Ar fraction $\text{Ar}/(\text{Ar} + \text{X})$ where $\text{X} = \text{N}_2$ or CO_2 . The pressure was fixed at 20 or 150 Pa, while the power was kept at 300 W. The total flow was 200 or 1000 sccm, with Ar and N_2 or CO_2 flows determined by the mixing ratio. The value for pure Ar compares well with the 1.4 eV seen by Godyak et al. for similar conditions ⁴¹. Especially in the case of dilute plasma (<10% CO_2), T_e depends strongly on the mixing ratio. At all conditions of flow and pressure the dilute mixture shows a dramatic decrease in T_e , with the lowest T_e at the highest pressure. Godyak et al. see a similar decrease in T_e for a pure Ar ICP plasma as a function of pressure, from 0.13 to 13 Pa ⁴¹.

Figure 2c shows the dependence of T_e on pressure for Ar, N_2 and CO_2 total flows of 100-200 sccm. T_e shows a rapid increase with pressure with constant input power for pure N_2 or CO_2 flows. The increase in T_e for CO_2 is counterintuitive. To confirm our measurement, we repeated these experiments with N_2 instead of CO_2 , noting similar trends. The same trends were also reported by Younus et al. for N_2 -Ar plasma at lower pressures ⁴³. Conversely, the T_e for a pure Ar flow decreases with increasing pressure.

The most interesting result is shown in Figure 2d, which shows the emission of the CO product and the conversion of CO_2 molecules as a function of pressure: The CO_2 conversion and the CO emission are both anti-correlated to the electron temperature, T_e (the maxima in Figure 2d occur at the same position at the minima in Figure 2c).

3.2 Conversion efficiency

Elsewhere, we studied energy and conversion efficiencies for pure CO_2 and CO_2 -Ar plasma with high CO_2 content ⁸. There, adding Ar to the plasma did increase the conversion efficiency and the energy efficiency. Here we studied the conversion efficiency of more dilute mixtures. Figure 2b shows that for these dilute mixtures T_e can vary significantly.

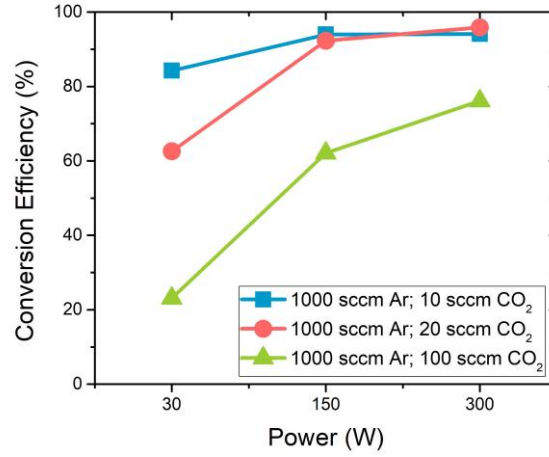


Figure 3. Conversion efficiency of CO₂ dissociation in RF plasma as a function of power for Ar-CO₂ mixtures, which are indicated in the figure. Pressure was fixed at 14 Pa.

The conversion efficiency was calculated using equation (1):

$$\chi = \frac{m_{CO_{out}}}{m_{CO_2 in}} \quad (1),$$

where $m_{CO_2 in}$ and $m_{CO_{out}}$ are the calibrated flow rates of carbon dioxide and carbon monoxide, respectively. Figure 3 shows the calculated conversion efficiencies (χ) versus power. The dilute mixtures show high conversions at low T_e values (see Figure 2b and Figure 3). The strong anti-correlation of T_e and CO₂ conversion is seen in Figures 2c and 2d respectively.

The energy efficiency for the conversion process is a typical figure of merit for plasma conversion. However, it is not very informative for a dilute plasma. For example, for the 300 W data at 1% dilution of CO₂ in Ar the specific energy deposited per Ar atom is 4.6 eV. If we assume that the CO₂ receives the same amount of energy, then the energy efficiency for full conversion of CO₂ is $2.9/4.6 \approx 60\%$. However, if we take it that all of the energy dissipated in the plasma is needed to convert this 1% of CO₂ the specific energy is 460 eV and the energy efficiency is below 1%. Such conditions are only of interest for scientific exploration.

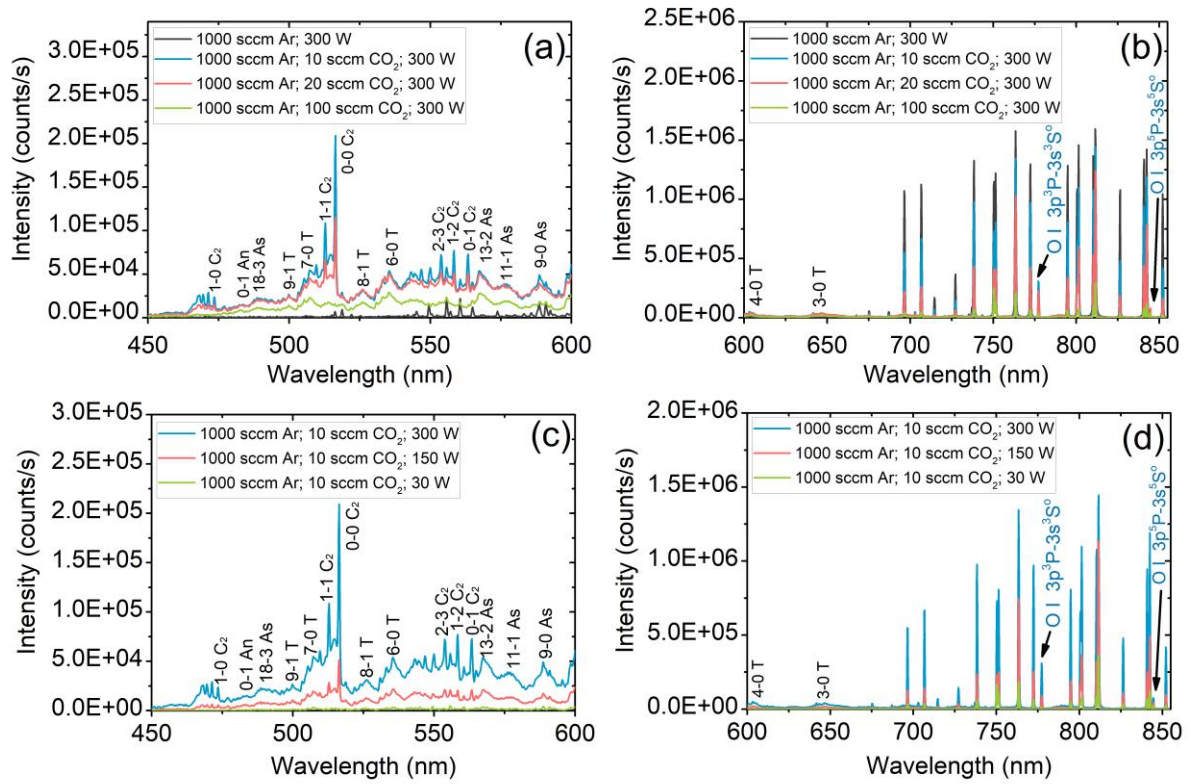


Figure 4. (a, b) Emission spectra from a pure Ar, and a CO₂ -Ar mixed plasma recorded at 14 Pa, 300 W RF power, for a CO₂ flow of 10 sccm, 20 sccm and 100 sccm, and an Ar flow of 1000 sccm. (a) wavelength range 450 - 600 nm. (b) wavelength range 675 – 855nm; (c, d) Emission spectra from CO₂ -Ar mixed plasma were recorded at 14 Pa for RF Power of 30 W, 150 W, 300 W. CO₂ flow and Ar flow were fixed at 10 sccm and 1000 sccm, respectively. (c) wavelength range 450 - 600 nm. (d) wavelength range 675 – 855 nm. Note the change in intensity scale.

3.3 Optical emission spectroscopy

Figure 4 shows the optical emission of CO₂-Ar mixtures gases plasma in three different CO₂ flows (10 sccm, 20 sccm and 100 sccm). The power, pressure and flow rate of Ar were fixed at 300 W, 14 Pa and 1000 sccm, respectively. The emission spectrum shows the emission from

C₂ (Swan band), CO (Ångstrom (An), Asundi (A) and Triplet bands (T)), Ar I (2p_y-1s_x) and O I multiplet (777 nm and 844 nm). When the CO₂ flow rate is set at 10 sccm, we see strong optical emission from C₂ Swan band system of the sequence ($\Delta v = 0, \pm 1$), see reference ⁴⁶. Transitions are labeled by v'-v'' C₂. Clear lines from CO bands have been labeled in a similar way. The transition frequencies were obtained from reference ³⁷. Figure 4b and Figure 4d show the oxygen I multiplet (777 nm and 844 nm) and the argon I atomic emission lines. These argon lines correspond to transitions from the 2p_y to 1s_x state ⁴⁷. Clearly, the emission of C₂ Swan and Ar I lines decreases significantly by adding more CO₂. When the CO₂ flow rate is up to 20 sccm we see a drastic reduction of the Swan band emission. At 100 sccm the emission of the C₂ Swan band disappears. In all cases the emission is superimposed on a broad CO₂ emission continuum, that cannot be clearly resolved ³⁷. The Swan band is visible only at the highest power and the highest dilutions (1-2%). Even for 10% CO₂ in Ar, we see only the CO emission, superimposed on a CO₂ background.

A more pronounced change of the Swan band emission is seen when the power is changed. Whereas the conversion reaches a plateau at 150 W, the C₂ Swan band emission still increases very significantly when the power is increased from 150 W to 300 W as seen in Figure S1 in the supporting information. Figure 4c shows the optical emission from 450–600 nm for three different power values (30, 150, 300 W). Only at the highest power and the highest dilution the Swan band emission is dominant. For lower power or higher CO₂ flow it is barely visible. Figure S1 shows that Swan band emission disappears for a high CO₂ concentration or T_e.

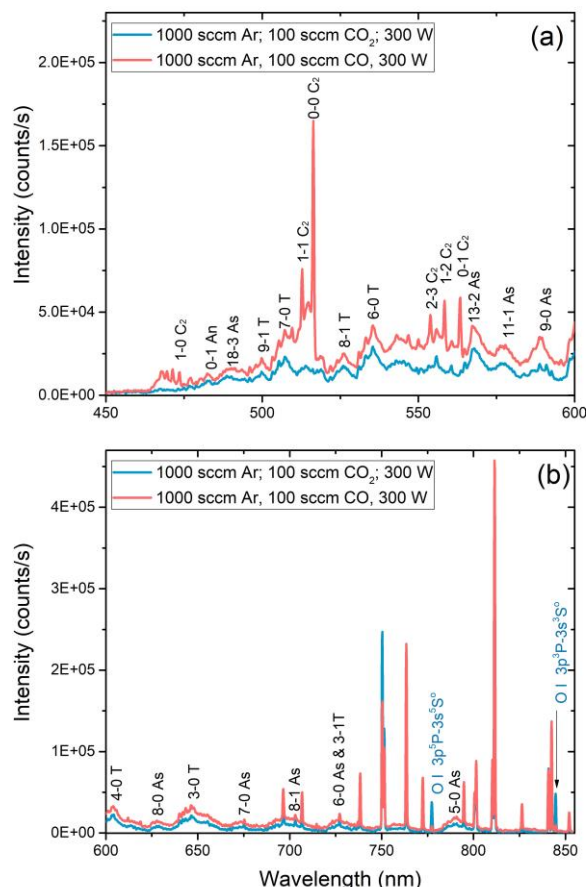


Figure 5. Emission spectra from CO-Ar (1:10) and CO₂-Ar (1:10) mix gases plasma recorded at 14 Pa, 300 W RF power and 1000 sccm Ar flow. **(a)** wavelength range 450 - 600 nm. **(b)** wavelength range 600 - 855 nm. The unassigned intense lines are Ar lines, not discussed in this paper. Note the change in intensity scale.

One remarkable feature (see Figure 4c) is the presence of very highly vibrationally excited CO molecules in the plasma. The 18-3 As line shows the presence of $v=18$ CO in the plasma. Although part of the vibrational excitation might be due to a shift in the excited state potential curves in the Franck-Condon region, an excitation of such high levels is rarely observed, as can be seen in the potential curves shown in Figure 11 of Rond et al.³⁷. These authors also observed highly vibrationally excited CO₂ in their RF torch. To study if the highly excited CO is formed

in the CO₂ dissociation process or is due to excitation of CO in the plasma, we ran experiments with CO instead of CO₂ feeding the plasma.

Figure 5 compares the emission spectra from both CO and CO₂ discharges diluted by Ar under similar conditions. For the same flow and dilution, the CO shows a stronger C₂ Swan band emission. The CO₂ background and the CO emission are comparable. However, the emission from O atoms is much stronger in the CO₂ than in the CO plasma. This indicates that the O density is much higher in the CO₂ plasma.

Figure 6 shows a series of spectra of undiluted CO and CO₂ plasma at different pressures. The intensity of the CO₂ emission background increases when the pressure decreases (the spectra are similar for the CO₂ and the CO plasma).

Interestingly, the CO₂ background – discussed in section 2.2 – is also visible in the spectra of the CO plasma. Clearly CO₂ is formed in the CO plasma. This implies that also C atoms and derivatives must be formed in the CO plasma. Indeed, after long experimental runs a slight blackening by C deposition of the system was observed for CO plasma operation, which was not observed earlier for a CO₂ plasma. In addition, the C₂ Swan band is invisible in CO₂ plasma and almost invisible in CO plasma. Only the 0-0 vibrational peak (516.4 nm) of the C₂ Swan band is observable in pure CO plasma. The constituent C-atoms must be formed by CO decomposition, as indicated in section 2.2. The absence of a Swan band emission in the undiluted CO₂ plasma at low pressure agrees with the data of Rond et al.³⁷.

Note that a CO emission of $v=19$ is observed. Clearly, the CO is very strongly vibrationally heated in both the CO and CO₂ plasma. This indicates that the vibrational excitation is due to excitation of CO in the plasma, for instance by ladder climbing. The vibrational excitation is not primarily caused by the CO₂ dissociation process.

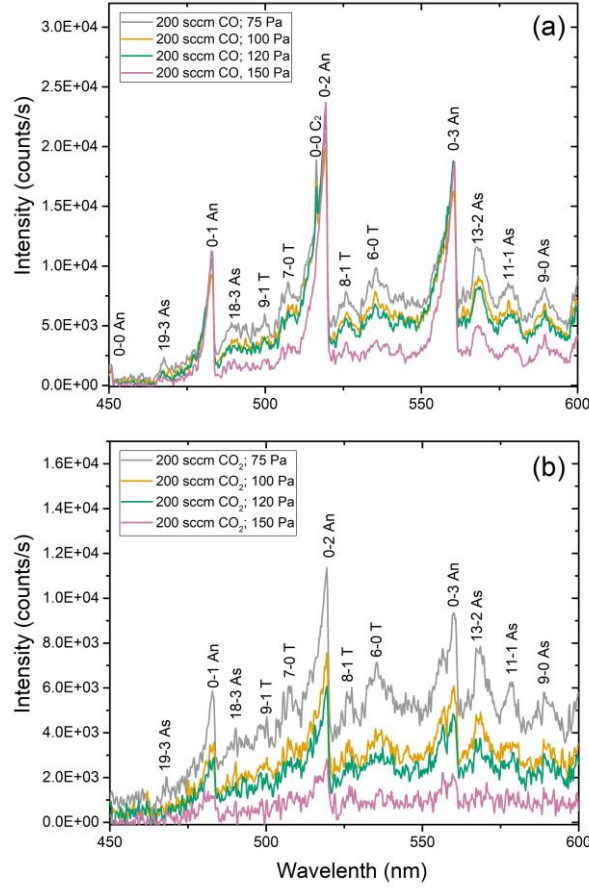


Figure 6. (a) Emission spectra of CO plasma at different pressures. Power and gas flow was fixed at 300 W and 200 sccm. **(b)** Emission spectra of CO₂ plasma at different pressures. Power and gas flow was fixed at 300 W and 200 sccm.

The correlation between T_e and conversion and between T_e and the nature of the optical emission spectra was already demonstrated in Figure 3 and Figure 4. In Figure 2c we show the relation between T_e and pressure. When CO₂ flow and RF power were fixed at 100 sccm and 150 W respectively, a minimum of $T_e \approx 2.5$ eV is seen. To examine if the CO₂ conversion follows this small changes of T_e with pressure, we have measured conversion as a function of pressure. The results are shown in Figure 2d. A clear anti-correlation with T_e is seen. Figure 2d also shows the intensity of a distinct emission line as a function of pressure. This line is

seen at 283 nm (the CO 3rd positive system) and is chosen, because it is well separated from the other lines (see Figure S2 in the supporting information). A maximum of CO production and CO emission is seen around the minimum of T_e . Figure S2 shows that such a maximum is also seen for other CO emission lines, as well as for O multiplet-emission lines. The pressure dependence of emission and conversion is very similar. Crudely speaking, the emission intensity is proportional to the conversion times the line excitation probability. The similarity of the curves in Figure 2d shows that the variation of the line excitation probability is not very sensitive to T_e .

Besides electrons, ions and neutrals also metastable excited atoms can be present in the plasma and play an important role, especially where T_e is concerned. Excited states of Ar are present as seen in the spectroscopic data in figures 4b+d, 5b and S1b+d. The Ar I lines observed are all due to radiative decay of Ar 3p⁵4p levels to 3p⁵4s levels⁴⁸. Some of the lower levels are metastable and do not decay⁴⁹. The metastable density has been measured by Yang et al. and is higher than the Ar⁺ ion density⁵⁰. In several studies on Ar containing ICP plasma the ratio of the Ar I lines at 811.5 and 750.4 nm is studied. Czerwicz & Graves (CG) find for pure Ar a one to one correlation of this ratio and T_e ⁴⁸. We find our pure Ar measurement in Fig 4b (1000 sccm Ar 300W) for the ratio $R=I(811.5)/I(750.5)$ $R=1.8$. The corresponding T_e value from fig 10 of the paper by CG is $T_e=1.0$ eV. The T_e seen in Figure 2c is about 1.7 eV. This difference is not so large considering the different experimental geometries, pressure and power (53 Pa & 50 W for CG versus 14 Pa & 300 W for the present data). The Ar-CO₂ mixtures from our data cannot be compared to the CG data.

The Ar I spectroscopy demonstrates that Ar* is present in the plasma. As Ar* has a low ionization potential of about 4.1 eV the metastables contribute strongly to sustain the Ar plasma at a low T_e by ionization by low energy electrons.

Metastable Ar can be efficiently quenched by CO₂ molecules. Sadeghi et al. found a cross section for de-excitation of Ar* of more than 100 Å²⁵¹. This is clearly visible in Fig. 4b, where the radiation at 750.5 nm, formed by excitation of Ar*, has dropped more than a factor of 5 with the addition of 10% CO₂. This implies rapid destruction of Ar* by adding CO₂. Thus a CO₂ admixture of a few percent will increase T_e because of two reasons: 1 – CO₂ quenches Ar*; 2 – CO₂⁺ undergoes facile dissociative recombination requiring a higher T_e to sustain the plasma.

4. DISCUSSION

4.1 Plasma conditions

Figure 2b shows that at large Ar fraction the T_e decreases strongly. Adding 2% CO_2 to pure Ar increases T_e by 3 eV at 150 Pa. This is caused by $\text{CO} + \text{O}$ formation from dissociative recombination of CO_2^+ and e^- occurs at a very high rate, much higher than recombination of Ar^+ and e^- for which a third body is needed. In addition, metastable Ar is efficiently quenched by CO_2 . Ar^* has a very low ionization energy and facilitates sustaining the plasma with relatively cold electrons. As a consequence the overall ionization lifetime decreases and the ionization rate should increase to sustain the plasma. This increase drives T_e up. A similar behaviour is seen for N_2 . At very low dilutions of Ar by CO_2 we therefore expect to see processes that are caused by low energy electrons. The processes that require a high T_e will be favored by pure CO_2 plasma or by plasma with a high CO_2 content. The biggest change in T_e occurs during the addition of the first few percent of CO_2 to an Ar plasma. The low T_e suggests that CO_2 dissociation is driven by ladder climbing involving electrons of energies from 0.5-4 eV⁷. Singh and Graves observed a small dip in their electron energy distribution function at about 2-3 eV with a T_e similar to that in the present work³¹.

The effect of plasma power on a pure Ar plasma is shown in Figure 2a. As the RF power is increasing T_e is slightly decreasing. At higher power the electron-electron collision frequency increases, which will exhaust the electrons with the highest energy⁵². Similar results were obtained by Nisha et al. in RF plasma, who observed a drop in T_e with increasing power⁴⁵. Consequently, in high power cases we expect processes requiring a low T_e .

4.2 CO_2 conversion

The conversion efficiencies in Figure 3 show a very strong correlation with the power and the CO_2 -Ar ratio. The lowest ratio combined with the highest power gives the highest

conversion. T_e is anti-correlated with the Ar content of the plasma and with the power, and strongly anti-correlated to the conversion, as shown in Figures 2c and 2d. The energy efficiency – hard to define here, as discussed – is getting worse with a more diluted plasma, and other methods should be used to decrease T_e for a practical reactor. Options that we are considering obtain an efficient reactor are addition of a catalytic convertor, suppression of recombination by shaping the plasma tube, working with a thermal arc having a low T_e , see e.g. ^{6, 53}.

4.3 Measurement of the CO bands.

CO emission from CO as source gas is easier to interpret than for CO₂ as source gas, because CO is added at room temperature. It is heated by electron impact and CO–CO collisions and cooled at the walls. Du et al. showed that the CO rotational temperature resulting from CO₂ dissociation is in equilibrium with the walls (at pressures significantly higher than ours) for a Dielectric Barrier Discharge ³³. Due to limited resolution we cannot measure the rotational bands. The vibrational bands show a different behaviour. The strongest lines are ones from the Ångström band starting from $v=0$. These CO molecules have collided with the wall and are vibrationally cold. Subsequently they are excited by hot plasma electrons into a radiative state. Just like in the case of rotation mentioned above, the vibrational quantum number will not change in the excitation and radiative de-excitation. Thus, the plasma contains significant amounts of vibrationally (and rotationally) cold CO. We also see a complex spectrum with lines corresponding to highly vibrationally excited molecules; in the Asundi band we see molecules with $v=19$. These molecules must be heated vibrationally inside the core of the plasma. Direct Franck-Condon excitation of those molecules by high energy electrons is unlikely. Indeed, vibrational ladder climbing can lead to very highly vibrationally excited CO when the molecules are heated by near IR lasers up to $v<7$ ¹⁹. We clearly observe CO molecules that are excited via a similar ladder climbing mechanism.

CO₂ plasma shows a lower emission intensity of CO, which has to be produced from CO₂ in the plasma (Figure 5a). The amount of CO OES from CO plasma is 2-3 times higher for an Ar diluted CO plasma than for the Ar diluted CO₂ one. The same is seen in Figure 6 for CO emission from pure CO and CO₂ plasma. The lower intensity for CO₂ plasma is reasonable, because the conversion of CO₂ to CO in the plasma is not 100% efficient. The spectra of CO generated in a CO₂ plasma also show lines from highly vibrationally excited states. Likewise Ångström band lines from $v=0$ are seen. CO is heated in the core of the plasma, but it can still quench on the walls before re-excitation. This yields a large spread in vibrational excitation. There is no significant difference between the CO spectra taken at different pressures in pure CO₂ plasma (Figure 6b). The vibrationally highly excited molecules do decrease in intensity with increasing pressure. This may reflect a more efficient cooling by the CO at the walls or a decrease of T_e . Since the vibrationally excited molecules are seen both in CO₂ plasma and CO plasma, they must form by direct electron excitation of CO molecules.

In Figure 6a, a significant background of CO₂* chemiluminescence is seen. We see that significant amounts of CO₂ are made in the CO plasma. The emission intensity of the Ångström band is increasing when increasing the pressure. However, the emission from Triplet and Asundi shows an opposite dependence on pressure. The upper electron state of Ångström (10.78eV) is much higher in excitation energy than Triplet's (6.92 eV) or Asundi (7.58 eV). This indicates that the decrease of relative intensity with pressure is due to a decreasing T_e , resulting in a relative decrease of high energy electrons (>8 eV) compared to the relative increase of low energy electrons (5-6 eV) ⁵⁴⁻⁵⁵.

4.4 Measurement of C₂ Swan band

We see a dramatic change in the spectra when the CO₂ flow becomes more diluted in Ar (see Figure 4a). At 100 sccm CO₂, we see mainly emission from CO, similar to that measured for in pure CO₂ and CO in Figure 6. In these cases we expect the same behavior, because the CO is

directly excited by hot plasma electrons⁵⁶. At severe dilution (range 2% - 1%), the T_e drops very quickly (Figure 2b). Therefore, the dominant optical emission is produced by processes that are driven by very low energy electrons. These are the C_2 Swan bands, with an excitation energy of only 2 eV.

As indicated in section 2.2, C_2 is formed in collisions between vibrationally excited CO molecules. Both IR radiation and low energy electrons can vibrationally excite the CO by so-called ladder climbing and bring it into a state that allows it to be reactive with another excited CO molecule to form C. Further collisions of C result into the formation of C_2 . Because the C_2 formation probability is at least quadratic versus the CO partial pressure, we expect more C_2 production from a pure CO plasma, than from producing CO through CO_2 plasma. This larger C_2 production in CO plasma is shown in Figure 5a.

But still in a CO_2 plasma, C_2 can be formed efficiently. This is shown in Figure 4. Reducing T_e by increasing CO_2 dilution results in the increased formation of the C_2 molecule. The T_e can also be reduced slightly by increasing the power. This is shown in Figure 2a. Consequently, one expects an increase in the Swan band emission with power, as seen in Figure 4c. In plasma with much higher power and pressure as seen in the work of Spencer and Gallimore and Bongers et al. also strong emission from the Swan bands is observed²⁶⁻²⁷. We believe this is due to the fact that at high power and high pressure the T_e is low and the CO bands cannot be excited. This in turn suggests that the CO_2 conversion should be high and that is indeed the case.

For highly diluted CO_2 and powers above 150 W the conversion of CO_2 exceeds 90%, for both the 1% and 2% mixtures. The conversion saturates, see Figure 3a. Also, the Swan band emission becomes prominent for these conditions. Nevertheless, the Swan band yield is not saturated as it is higher for the 1% mixture compared to the 2% case (see Figure 4a) while the CO concentrations are likely higher for the 2% dilution, so the increased yield of the Swan band emission for the 1% mixture must be due to a higher excitation probability, which is connected

to the lower T_e . Also, the increase in Swan band emission with increasing power (Figure 4c) shows that emission does not saturate due to an increasing excitation probability.

C_2 is formed from CO and that should be easier for pure CO than for CO_2 as feed gas. Given the saturation in CO production for a 1 or 2% diluted CO_2 -Ar plasma shown in Figure 3, the C_2 yields should be similar for CO_2 and CO plasma. However, for the 10% CO_2 -Ar data in Figure 5a saturation in CO production with power has not yet been achieved (shown in Figure 3), which explains the higher Swan band emission for CO in Figure 5a. Besides the quadratic CO pressure dependence, another factor in the C_2 production is the destruction of C_2 by the O atoms. The O emission line is much stronger in CO_2 plasma (Figure 5b) at the same conditions. It indicates that there are more oxygen atoms in the CO_2 plasma than in the CO plasma. Thus, the destruction process is more prominent for a CO_2 plasma than for a CO plasma, yielding a lower emission from the C_2 Swan band.

5. CONCLUSION

We show that adding Ar to a CO_2 plasma can change the characteristics of the plasma dramatically. Measurements with a Langmuir double probe show that T_e changes dramatically as a function of the settings, notably the Ar/ CO_2 ratio. We have found a strong anti-correlation of CO_2 conversion efficiency with T_e . A similar dependence of the OES with T_e was also observed. Low T_e (≈ 2 eV) leads to significant Swan band emission, whereas higher T_e favors emission from the CO bands. Ångström band emission is favored at the highest T_e . We observed a strong anti-correlation between T_e and the intensity of the optical emission spectroscopy of product CO lines, most dramatically shown in Figure 2d. A T_e as low as possible is required to obtain a high CO_2 conversion. This is a very important consideration - but not the only one - when designing future reactors, and a benchmark for modeling of the processes involved.

We have not analyzed our results in terms of vibrational temperatures. However, we note that equilibrium between the C_2 vibrations and those of CO_2 is not obvious, given the complex production process of C_2 and the different behavior of Swan band emission in CO and CO_2 plasma. We do observe $v=19$ in CO but not in C_2 . This strongly suggests that T_{vib} is not the same for CO and C_2 and presumably it will be different for CO_2 too. Thus, the C_2 Swan band emission occurs at the end of a long sequence of reactions and does not reflect the internal state of the CO_2 that is excited by the plasma, by ladder climbing or by hot electron impact. C_2 Swan band emission is an indicator of low T_e , where the plasma cannot electronically excite CO.

In summary, high CO_2 conversion requires a low T_e . Such a low T_e results in efficient Swan band emission. It is unlikely that the T_{vib} measured for C_2 is the same as that of CO_2 .

ACKNOWLEDGMENTS

This work was supported by the National Natural Science Foundation of China (Grant No. 51561135013 and 21603202) and The Netherlands Organization for Scientific Research (NWO) - grant registration number: CHINA.15.119

Supporting information

Two figures are added: Figure S1 shows additional optical emission spectra; Figure S2 shows the pressure dependence of several CO and O-atom emission lines.

REFERENCES

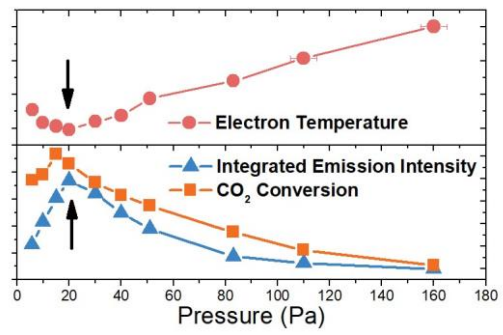
1. Lebouvier, A.; Iwarere, S. A.; d'Argenlieu, P.; Ramjugernath, D.; Fulcheri, L., Assessment of Carbon Dioxide Dissociation as a New Route for Syngas Production: A Comparative Review and Potential of Plasma-Based Technologies. *Energy Fuels* **2013**, *27*, 2712-2722.
2. Hartley, P.; Medlock, K. B.; Temzelides, T.; Zhang, X. Y., Energy Sector Innovation and Growth: An Optimal Energy Crisis. *Energy J.* **2016**, *37*, 233-290.

3. Martens, J. A.; Bogaerts, A.; De Kimpe, N.; Jacobs, P. A.; Marin, G. B.; Rabaey, K.; Saeys, M.; Verhelst, S., The Chemical Route to a Carbon Dioxide Neutral World. *ChemSusChem* **2017**, *10*, 1039-1055.
4. Wilson, I. A. G.; Styring, P., Why Synthetic Fuels Are Necessary in Future Energy Systems. *Front. Energy Res.* **2017**, *5*, 10.
5. Snoeckx, R.; Bogaerts, A., Plasma Technology - a Novel Solution for CO₂ Conversion? *Chem. Soc. Rev.* **2017**, *46*, 5805-5863.
6. Ashford, B.; Tu, X., Non-Thermal Plasma Technology for the Conversion of Co₂. *Curr. Opin. Green Sustain. Chem.* **2017**, *3*, 45-49.
7. Fridman, A., *Plasma Chemistry*; Cambridge University Press: New York, 2008.
8. Huang, Q.; Zhang, D. Y.; Wang, D. P.; Liu, K. Z.; Kleyn, A. W., Carbon Dioxide Dissociation in Non-Thermal Radiofrequency and Microwave Plasma. *Journal of Physics D-Applied Physics* **2017**, *50*, 6.
9. Spencer, L. F.; Gallimore, A. D., Efficiency of Co₂ Dissociation in a Radio-Frequency Discharge. *Plasma Chemistry and Plasma Processing* **2011**, *31*, 79-89.
10. Savinov, S. Y.; Lee, H.; Song, H. K.; Na, B. K., A Kinetic Study on the Conversion of Methane to Higher Hydrocarbons in a Radio-Frequency Discharge. *Korean J. Chem. Eng.* **2004**, *21*, 601-610.
11. Savinov, S. Y.; Lee, H.; Song, H. K.; Na, B. K., Decomposition of Methane and Carbon Dioxide in a Radio-Frequency Discharge. *Ind. Eng. Chem. Res.* **1999**, *38*, 2540-2547.
12. Piejak, R. B.; Godyak, V. A.; Alexandrovich, B. M., A Simple Analysis of an Inductive Rf Discharge. *Plasma Sources Science & Technology* **1992**, *1*, 179-186.
13. Rusanov, V. D.; Fridman, A. A.; Sholin, G. V., Physics of Chemically Active Plasma with a Non-Equilibrium Vibrational Excitation of Molecules. *Uspekhi Fiz. Nauk* **1981**, *134*, 185-235.
14. van Rooij, G. J.; van den Bekerom, D. C. M.; den Harder, N.; Minea, T.; Berden, G.; Bongers, W. A.; Engeln, R.; Graswinckel, M. F.; Zoethout, E.; de Sandena, M., Taming Microwave Plasma to Beat Thermodynamics in Co₂ Dissociation. *Faraday Discuss.* **2015**, *183*, 233-248.
15. Tao, X. M.; Bai, M. G.; Li, X. A.; Long, H. L.; Shang, S. Y.; Yin, Y. X.; Dai, X. Y., Ch₄-Co₂ Reforming by Plasma - Challenges and Opportunities. *Prog. Energy Combust. Sci.* **2011**, *37*, 113-124.
16. Neyts, E. C.; Bogaerts, A., Understanding Plasma Catalysis through Modelling and Simulation-a Review. *Journal of Physics D-Applied Physics* **2014**, *47*, 224010.
17. Aerts, R.; Martens, T.; Bogaerts, A., Influence of Vibrational States on Co₂ Splitting by Dielectric Barrier Discharges. *J. Phys. Chem. C* **2012**, *116*, 23257-23273.
18. Nunnally, T.; Gutsol, K.; Rabinovich, A.; Fridman, A.; Gutsol, A.; Kemoun, A., Dissociation of Co₂ in a Low Current Gliding Arc Plasmatron. *Journal of Physics D-Applied Physics* **2011**, *44*, 7.
19. Martin, J. P.; Perrin, M. Y.; Porshnev, P. I., Co₂ Formation in an Optically Excited V-V up-Pumped Co Flow. *Chem. Phys. Lett.* **2000**, *332*, 283-289.
20. Bogaerts, A.; Kozak, T.; van Laer, K.; Snoeckx, R., Plasma-Based Conversion of Co₂: Current Status and Future Challenges. *Faraday Discuss.* **2015**, *183*, 217-232.
21. Klarenaar, B. L. M.; Engeln, R.; van den Bekerom, D. C. M.; van de Sanden, M. C. M.; Morillo-Candas, A. S.; Guaitella, O., Time Evolution of Vibrational Temperatures in a Co₂ Glow Discharge Measured with Infrared Absorption Spectroscopy. *Plasma Sources Science & Technology* **2017**, *26*, 11.
22. Juurlink, L. B. F.; Killelea, D. R.; Utz, A. L., State-Resolved Probes of Methane Dissociation Dynamics. *Prog. Surf. Sci.* **2009**, *84*, 69-134.

23. Jiang, B.; Guo, H., Communication: Enhanced Dissociative Chemisorption of CO_2 Via Vibrational Excitation. *J. Chem. Phys.* **2016**, *144*, 5.
24. van Rooij, G. J.; Akse, H. N.; Bongers, W. A.; van de Sanden, M. C. M., Plasma for Electrification of Chemical Industry: A Case Study on CO_2 Reduction. *Plasma Phys. Control. Fusion* **2018**, *60*, 7.
25. Ma, J.; Pu, Y. K., Tuning the Electron Temperature of a Nitrogen Plasma by Adding Helium and Argon. *Physics of Plasmas* **2003**, *10*, 4118-4122.
26. Spencer, L. F.; Gallimore, A. D., CO_2 Dissociation in an Atmospheric Pressure Plasma/Catalyst System: A Study of Efficiency. *Plasma Sources Science & Technology* **2013**, *22*.
27. Bongers, W., et al., Plasma-Driven Dissociation of CO_2 for Fuel Synthesis. *Plasma Process. Polym.* **2017**, *14*, 8.
28. Nguyen, S. V. T.; Foster, J. E.; Gallimore, A. D., Operating a Radio-Frequency Plasma Source on Water Vapor. *Rev. Sci. Instrum.* **2009**, *80*, 8.
29. Rousseau, A.; Teboul, E.; Bechu, S., Comparison between Langmuir Probe and Microwave Autointerferometry Measurements at Intermediate Pressure in an Argon Surface Wave Discharge. *J. Appl. Phys.* **2005**, *98*, 9.
30. Chang, J. S.; Laframboise, J. G., Double-Probe Theory for a Continuum Low-Density Plasma. *Journal of Physics D-Applied Physics* **1976**, *9*, 1699-1703.
31. Singh, H.; Graves, D. B., Measurements of the Electron Energy Distribution Function in Molecular Gases in a Shielded Inductively Coupled Plasma. *J. Appl. Phys.* **2000**, *88*, 3889-3898.
32. Luo, D. B.; Ma, D. C.; He, Y.; Li, X. S.; Wang, S.; Duan, Y. X., Needle Electrode-Based Microplasma Formed in a Cavity Chamber for Optical Emission Spectrometric Detection of Volatile Organic Compounds through a Filter Paper Sampling. *Microchem J.* **2017**, *130*, 33-39.
33. Du, Y. J.; Tamura, K.; Moore, S.; Peng, Z. M.; Nozaki, T.; Bruggeman, P. J., Co Angstrom System for Gas Temperature Measurements in CO_2 Containing Plasmas. *Plasma Chemistry and Plasma Processing* **2017**, *37*, 29-41.
34. Munoz, J.; Dimitrijevic, M. S.; Yubero, C.; Calzada, M. D., Using the Van Der Waals Broadening of Spectral Atomic Lines to Measure the Gas Temperature of an Argon-Helium Microwave Plasma at Atmospheric Pressure. *Spectroc. Acta Pt. B-Atom. Spectr.* **2009**, *64*, 167-172.
35. Bond, J. R.; Gray, P.; Griffiths, J. F., Oscillations, Glow and Ignition in Carbon-Monoxide Oxidation - 1 - Glow and Ignition in a Closed Reaction Vessel and the Effect of Added Hydrogen. *Proc. R. Soc. London Ser. A-Math. Phys. Eng. Sci.* **1981**, *375*, 43-64.
36. Samaniego, J. M.; Egolfopoulos, F. N.; Bowman, C. T., CO_2^* Chemiluminescence in Premixed Flames. *Combust. Sci. Technol.* **1995**, *109*, 183-203.
37. Rond, C.; Bultel, A.; Boubert, P.; Cheron, B. G., Spectroscopic Measurements of Nonequilibrium CO_2 Plasma in Rf Torch. *Chem. Phys.* **2008**, *354*, 16-26.
38. da Silva, M. L.; Vacher, D.; Dudeck, M.; Andre, P.; Faure, G., Radiation from an Equilibrium $\text{CO}_2\text{-N}_2$ Plasma in the 250-850 Nm Spectral Region: Ii. Spectral Modelling. *Plasma Sources Science & Technology* **2008**, *17*, 9.
39. Wallaart, H. L.; Piar, B.; Perrin, M. Y.; Martin, J. P., C_2 Formation in Vibrationally Excited Co. *Chem. Phys. Lett.* **1995**, *246*, 587-593.
40. Babou, Y.; Riviere, P.; Perrin, M. Y.; Soufiani, A., Spectroscopic Study of Microwave Plasmas of Co(2) and Co(2)-N(2) Mixtures at Atmospheric Pressure. *Plasma Sources Science & Technology* **2008**, *17*, 11.

41. Godyak, V. A.; Piejak, R. B.; Alexandrovich, B. M., Electron Energy Distribution Function Measurements and Plasma Parameters in Inductively Coupled Argon Plasma. *Plasma Sources Science & Technology* **2002**, *11*, 525-543.
42. Hopwood, J.; Guarnieri, C. R.; Whitehair, S. J.; Cuomo, J. J., Langmuir Probe Measurements of a Radio-Frequency Induction Plasma. *J. Vac. Sci. Technol. A-Vac. Surf. Films* **1993**, *11*, 152-156.
43. Younus, M.; Rehman, N. U.; Shafiq, M.; Naeem, M.; Zaka-Ul-Islam, M.; Zakaullah, M., Evolution of Plasma Parameters in an Ar-N₂/He Inductive Plasma Source with Magnetic Pole Enhancement. *Plasma Sci. Technol.* **2017**, *19*, 9.
44. Vargheese, K. D.; Rao, G. M., Electron Cyclotron Resonance Plasma Source for Ion Assisted Deposition of Thin Films. *Rev. Sci. Instrum.* **2000**, *71*, 467-472.
45. Nisha, M.; Saji, K. J.; Ajimsha, R. S.; Joshy, N. V.; Jayaraj, M. K., Characterization of Radio Frequency Plasma Using Langmuir Probe and Optical Emission Spectroscopy. *J. Appl. Phys.* **2006**, *99*, 4.
46. Tanabashi, A.; Hirao, T.; Amano, T.; Bernath, P. F., The Swan System of C-2: A Global Analysis of Fourier Transform Emission Spectra (Vol 169, Pg 472, 2007). *Astrophys. J. Suppl. Ser.* **2007**, *170*, 261-261.
47. Kramida, A.; Ralchenko, Y.; Reader, J.; Team, N. A. Nist Atomic Spectra Database (Version 5.5.1), [Online].
48. Czerwicz, T.; Graves, D. B., Mode Transitions in Low Pressure Rare Gas Cylindrical Icp Discharge Studied by Optical Emission Spectroscopy. *Journal of Physics D-Applied Physics* **2004**, *37*, 2827-2840.
49. Boffard, J. B.; Jung, R. O.; Lin, C. C.; Wendt, A. E., Measurement of Metastable and Resonance Level Densities in Rare-Gas Plasmas by Optical Emission Spectroscopy. *Plasma Sources Science & Technology* **2009**, *18*, 11.
50. Yang, J.; Wu, A. J.; Li, X. D.; Liu, Y.; Zhu, F. S.; Chen, Z. L.; Yan, J. H.; Chen, R. J.; Shen, W. J., Experimental and Simulation Investigation of Electrical and Plasma Parameters in a Low Pressure Inductively Coupled Argon Plasma. *Plasma Sci. Technol.* **2017**, *19*, 11.
51. Sadeghi, N.; Setser, D. W.; Francis, A.; Czarnetzki, U.; Dobeles, H. F., Quenching Rate Constants for Reactions of Ar(4p ¹/₂ (0), 4p ¹/₂ (0), 4p ³/₂ (2), and 4p ⁵/₂ (2)) Atoms with 22 Reagent Gases. *J. Chem. Phys.* **2001**, *115*, 3144-3154.
52. Pu, Y. K.; Guo, Z. G.; Kang, Z. D.; Ma, J.; Guan, Z. C.; Zhang, G. Y.; Wang, E. G., Comparative Characterization of High-Density Plasma Reactors Using Emission Spectroscopy from Vuv to Nir. *Pure Appl. Chem.* **2002**, *74*, 459-464.
53. Li, J.; Zhang, X. Q.; Shen, J.; Ran, T. C.; Chen, P.; Yin, Y. X., Dissociation of Co₂ by Thermal Plasma with Contracting Nozzle Quenching. *J. CO₂ Util.* **2017**, *21*, 72-76.
54. El-Fayoumi, I. M.; Jones, I. R.; Turner, M. M., Hysteresis in the E- to H-Mode Transition in a Planar Coil, Inductively Coupled Rf Argon Discharge. *Journal of Physics D-Applied Physics* **1998**, *31*, 3082-3094.
55. Kang, N. J.; Oh, S.; Ricard, A., Determination of the Electron Temperature in a Planar Inductive Argon Plasma with Emission Spectroscopy and Electrostatic Probe. *Journal of Physics D-Applied Physics* **2008**, *41*, 6.
56. Fujimoto, T., Kinetics of Ionization-Recombination of a Plasma and Population-Density of Excited Ions - 2 - Ionizing Plasma. *Journal of the Physical Society of Japan* **1979**, *47*, 273-281.

TOC entry:



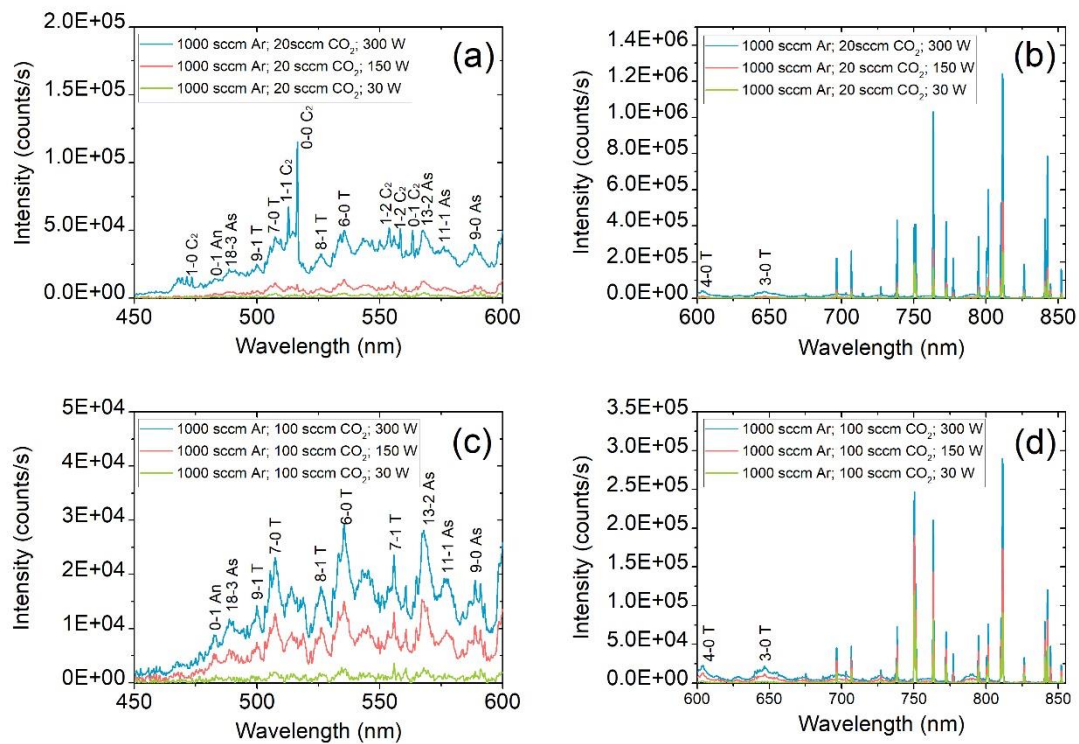


Figure S1 Emission spectrum from CO₂-Ar mixed plasma recorded at different supplied power (30 W, 150 W, 300 W). The Ar flow was fixed at 1000 sccm and CO₂ flow was fixed at 20 sccm and 100 sccm, respectively. The pressure was fixed at 14 ± 1 Pa.

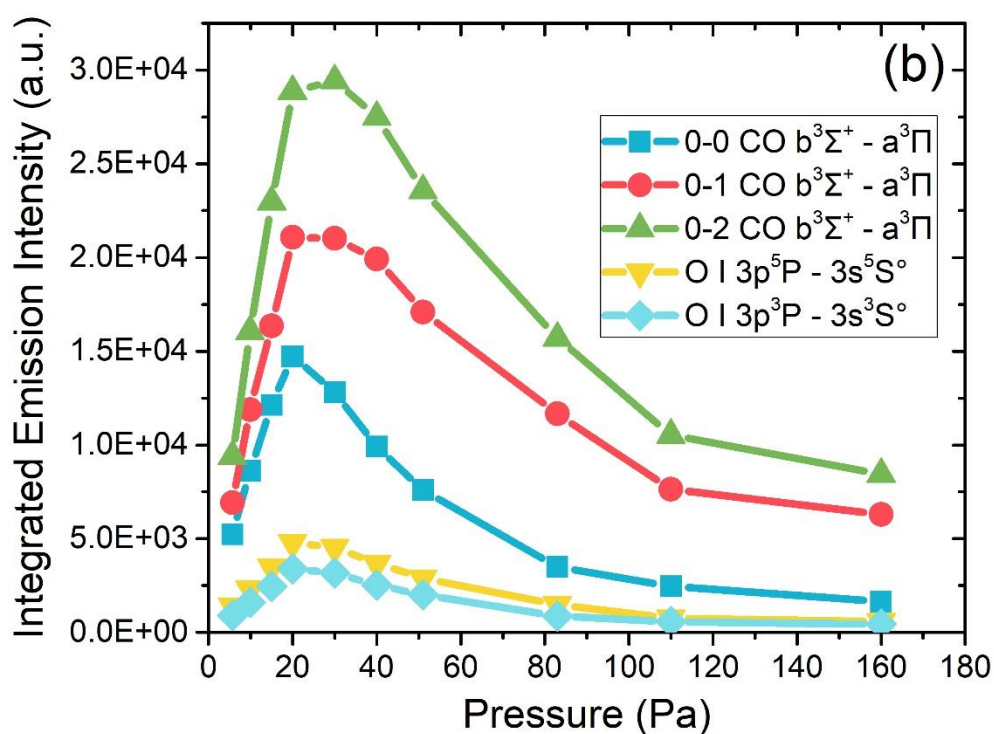
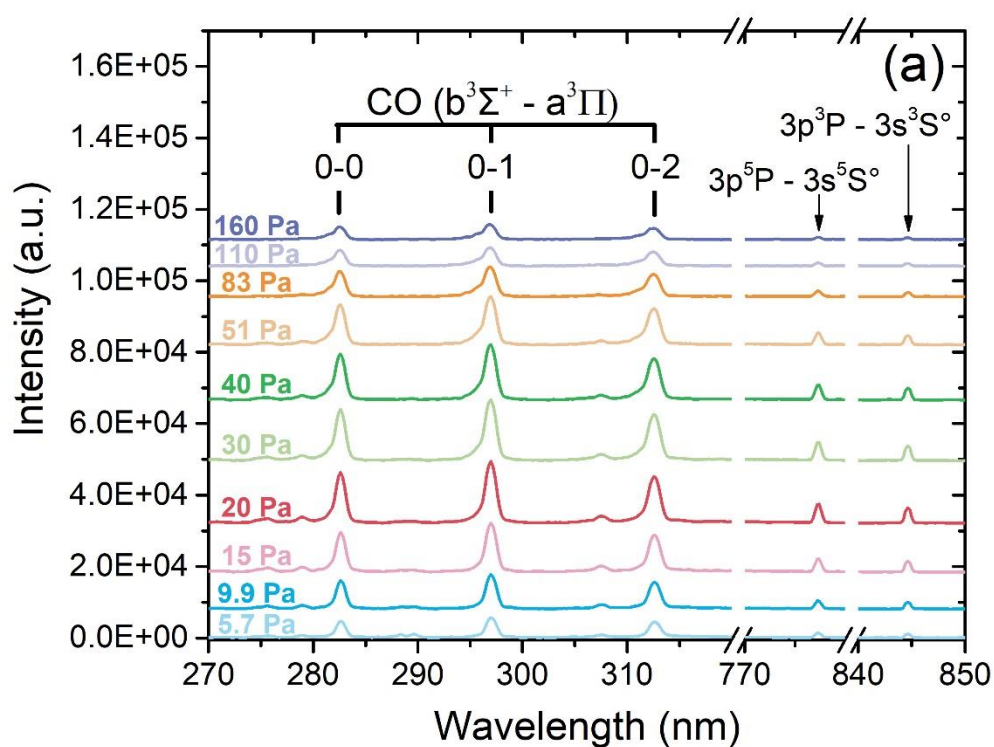


Figure S2 a) Emission spectrum of the CO $b^3\Sigma^+ - a^3\Pi$, O I $3p^5P \rightarrow 3s^5S^\circ$ (777 nm) and O I $3p^3P \rightarrow 3s^3S^\circ$ (844 nm) transitions at different pressure. b) integrated emission intensity of 0-0, 0-1, 0-2 transition of CO ($b^3\Sigma^+ - a^3\Pi$) system and O I ($3p^5P \rightarrow 3s^5S^\circ$, $3p^3P \rightarrow 3s^3S^\circ$).